Imprinting Structural Information from a GpG Ligand into the Configuration of a Chiral Diamine Ligand through Second-Sphere Communication in Platinum(II) Complexes

Kevin M. Williams,[†] Tommaso Scarcia,[‡] Giovanni Natile,*[,§,||] and Luigi G. Marzilli*[,†,⊥]

Department of Chemistry, Emory University, Atlanta, Georgia 30322, C.I.R.C.M.S.B., Università di Bari, via Celso Ulpiani 27, 70125 Bari, Italy, and Dipartimento Farmaco-Chimico, Università di Bari, via E. Orabona 4, 70125 Bari, Italy

Received January 20, 2000

Cisplatin forms the *cis*-Pt(NH_3)$_2$(d(GpG)) cross-link with DNA. We have recently created novel d(GpG) conformations by using "retro models" (complexes having bulky carrier ligands designed to slow d(GpG) dynamic motion). Our results define four conformer classes: HH1, HH2, ΔHT1, and ΛHT2, with a head-to-head or head-to-tail base orientation and a phosphodiester backbone with a normal (1) or opposite (2) propagation direction. Moreover, each G residue can be *syn* or *anti*, and the base canting can be left-handed (L) or right-handed (R). Thus, 32 variants of *cis*-Pt(NH_3)$_2$(d(GpG)) are conceivable, but the adduct is too dynamic to study. Thus far, by using retro models, we have obtained evidence for five variants with d(GpG) but only four with GpG. We therefore selected **Me$_2$DAP**Pt(GpG) complexes for study by ^{1}H and ^{31}P NMR spectroscopy, CD spectroscopy, and molecular mechanics and dynamics (MMD) calculations. Coordinated **Me$_2$DAP** (*N*,*N*′-dimethyl-2,4-diaminopentane) has N, C, C, N chiral centers designated, for example, as *R*,*R*,*R*,*R*. This ligand has greater flexibility and more readily inverted N centers than ligands used previously in GpG retro models. One goal was to determine whether the GpG ligand can control the configuration of a carrier ligand. (*R*,*R*,*R*,*R*)-**Me$_2$DAP**Pt(GpG) forms the *anti*, *anti* HH1 R variant almost exclusively. Equal populations of the two possible linkage isomers of (*S*,*R*,*R*,*R*)-**Me$_2$DAP**Pt(GpG) are formed, both favoring the *anti*, *anti* HH1 R variant; however, the isomer with the 5′-G *cis* to the *S* nitrogen has sharper signals, suggesting that interligand interactions are more favorable. Indeed, this linkage isomer was the major product of isomerization when (*R*,*R*,*R*,*R*)-**Me$_2$DAP**Pt(GpG) was kept at pH ∼9.5 to allow N center equilibration. Steric clashes between the **Me$_2$DAP** C−Me groups and the G O6 atoms found by MMD calculations appear to disfavor the HH1 conformer of (*S*,*S*,*S*,*S*)-**Me$_2$DAP**Pt(GpG) and (*S*,*S*,*S*,*R*)-**Me$_2$DAP**Pt(GpG) complexes. These two complexes have a significant population of the *anti*, *syn* ΔHT1 conformer, as indicated by broad ^{1}H NMR signals and by ^{31}P NMR and CD data. Equilibration of (*S*,*S*,*S*,*R*)-**Me$_2$DAP**Pt(GpG) at pH 9.5 leads to a mixture of (*S*,*S*,*S*,*S*)-**Me$_2$DAP**Pt(GpG) and at least one isomer of (*S*,*S*,*S*,*R*)-**Me$_2$DAP**Pt(GpG). Thus, second-sphere communication (hydrogen bonding and steric interligand interactions) influences both GpG conformation and **Me$_2$DAP** configuration.

Introduction

Cisplatin (*cis*-Pt(NH_3)$_2$Cl$_2$) is widely used as an anticancer drug; however, analogues of the type *cis*-PtX$_2$A$_2$ [X$_2$ = leaving ligands, A$_2$ = two unidentate or one bidentate amine ligand] are generally less active.[1,2] These agents bind primarily to the N7 of guanine bases (Figure 1), with the N7 of adenine a secondary target. The primary adduct that is formed by cisplatin is a 1,2-intrastrand cross-link between the N7 atoms of adjacent guanines; this type of adduct is thought to be responsible for the anticancer activity.

NMR spectroscopy has been used extensively to characterize oligonucleotide models of Pt−DNA adducts.[1] However, we have noted that the "dynamic motion problem" complicates the interpretation of the NMR spectra.[1,3−5] When all nuclei of a given species are unique, multiple conformations in fast exchange on the NMR time scale cannot be distinguished from one dominant conformation; one set of resonances is expected for either case. Furthermore, for rapidly interchanging conformers, coupling constants and chemical shifts will have values reflecting the weighted average for each conformer, but nuclear Overhauser effect (NOE) cross-peak intensities will be biased toward the conformer with the shortest distance between nuclei.

cis-Pt(NH_3)$_2$(GpG) and *cis*-Pt(NH_3)$_2$(d(GpG)) complexes, the simplest G-linked models of the major cisplatin−DNA adduct, have been characterized by a number of techniques, including CD spectroscopy,[6,7] ^{1}H NMR spectroscopy,[6−8] and molecular

[†] Emory University.
[‡] C.I.R.C.M.S.B., Università di Bari.
[§] Dipartimento Farmaco-Chimico, Università di Bari.
[||] E-mail: natile@farmchim.uniba.it.
[⊥] E-mail: lmarzil@emory.edu.

(1) Ano, S. O.; Kuklenyik, Z.; Marzilli, L. G. In *Cisplatin: Chemistry and Biochemistry of a Leading Anticancer Drug*; Lippert, B., Ed.; Wiley-VCH: Weinheim, 1999; pp 247−291.
(2) Jamieson, E. R.; Lippard, S. J. *Chem. Rev.* **1999**, *99*, 2467−2498.
(3) Ano, S. O.; Intini, F. P.; Natile, G.; Marzilli, L. G. *J. Am. Chem. Soc.* **1998**, *120*, 12017−12022.
(4) Marzilli, L. G.; Ano, S. O.; Intini, F. P.; Natile, G. *J. Am. Chem. Soc.* **1999**, *121*, 9133−9142.
(5) Williams, K. M.; Cerasino, L.; Natile, G.; Marzilli, L. G. *J. Am Chem. Soc.* **2000**, *122*, 8021−8030.
(6) Chottard, J.-C.; Girault, J.-P.; Chottard, G.; Lallemand, J.-Y.; Mansuy, D. *J. Am. Chem. Soc.* **1980**, *102*, 5565−5572.
(7) Girault, J.-P.; Chottard, G.; Lallemand, J.-Y.; Chottard, J.-C. *Biochemistry* **1982**, *21*, 1352−1356.
(8) den Hartog, J. H. J.; Altona, C.; Chottard, J.-C.; Girault, J.-P.; Lallemand, J.-Y.; de Leeuw, F. A. A. M.; Marcelis, A. T. M.; Reedijk, J. *Nucleic Acids Res.* **1982**, *10*, 4715−4730.

10.1021/ic000067n CCC: $20.00
Published on Web 12/19/2000

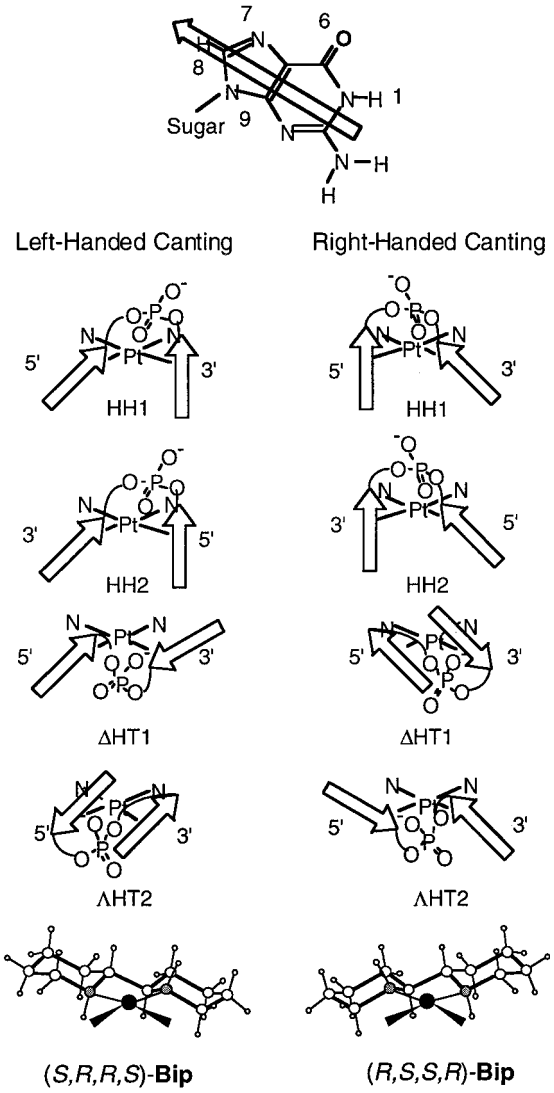

Figure 1. (Top) Guanine base with partial numbering scheme and with arrow designating base orientation. (Middle) Shorthand representations of the HH1, HH2, ΔHT1, and ΛHT2 conformers of N7−Pt−N7 cross-links in which the bases are head-to-head or head-to-tail and the propagation direction of the phosphodiester back-bond is normal (1) or opposite (2) that of B-DNA, with both left-handed (L) and right-handed (R) canting. (Bottom) (*S*,*R*,*R*,*S*)-**Bip** and (*R*,*S*,*S*,*R*)-**Bip** carrier ligands. For clarity, the remaining coordination positions are not shown.

modeling.[9] On the basis of the observation that both nucleotides of each complex were *anti*,[6] the cross-links were initially assigned structures in the HH1 conformer class (Figure 1). Studies of retro models (see below) show that there are three other classes, namely, HH2, ΔHT1, and ΛHT2 (Figure 1). Members of adjacent classes are separated by rotation of one G base about its Pt−N7 bond. Moreover, the G nucleotides can adopt *syn* or *anti* conformations, and the bases can have right-handed (R) or left-handed (L) canting (Figure 1). The 32 conceivable forms, which may not all be in a local miminum and which are therefore referred to as variants, are designated by the 5′-, then the 3′-G conformation, e.g., *anti*, *anti* HH1 R. *cis*-PtA_2**G**$_2$ adducts (**G** = N9-substituted guanine base that is not linked to another guanine) have for many years been known to favor HT orientations.[10,11] When nonbulky amine ligands are used, *cis*-PtA_2**G**$_2$ adducts have one set of time-averaged ^{1}H NMR signals due to rapid rotation around the Pt−N7 bond.[10,12]

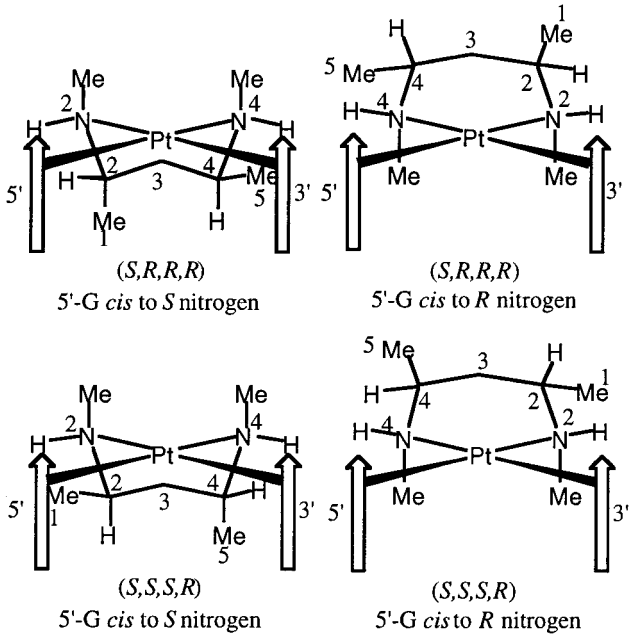

Figure 2. Isomers of (*S*,*R*,*R*,*R*)- and (*S*,*S*,*S*,*R*)-**Me$_2$DAP**Pt(GpG) in which GpG is in the HH1 conformation and **Me$_2$DAP** is in the *δ*-chair conformation. For clarity, the phosphodiester backbone is not shown.

Cisplatin is a very simple molecule, but the possibility of dynamic motion in cisplatin−DNA adducts complicates spectroscopic analysis. Thus, we have constructed analogues of cisplatin with bulky carrier ligands designed to reduce the dynamic motion. We have introduced the term "retro-modeling" to emphasize that our models are more complicated than the relevant molecule.[13] Most retro-model complexes we use have diamine carrier ligands with four chiral centers, two nitrogen atoms, and two carbon atoms, e.g., **Bip** and **Me$_2$DAP** [**Bip** = 2,2′-bipiperidine (Figure 1) and **Me$_2$DAP** = *N*,*N*′-dimethyl-2,4-diaminopentane (Figures 2 and 3)]. The uncoordinated ligands have fixed chiralities at the two carbon atoms. However, the chiralities of the nitrogen centers in the uncoordinated ligand rapidly invert because of the presence of a lone pair of electrons.[14,15] Thus, only three isomers of the diamine can be isolated. Two isomers are enantiomers, with *R*,*R* and *S*,*S* carbon chiralities. When coordinated, each of the two enantiomers could adopt up to three distinct configurations differing in N chirality. The configuration of the coordinated ligand is designated by the chirality of the N,C,C and N centers. For the *R*,*R* diamine, the three distinct configurations are *S*,*R*,*R*,*S*, *R*,*R*,*R*,*S*, and *R*,*R*,*R*,*R*. The *R*,*R*,*R*,*S* configuration is not C_2 symmetrical. The third ligand isomer (the *R*,*S* meso form) could coordinate with any of four non-C_2-symmetrical configurations. Because the chiral GpG ligand is directional, having a 5′-G and a 3′-G, multiple isomers of GpG adducts with complicated NMR spectra result when the diamine carrier ligand is not C_2 symmetrical.

Coordination of the *R*,*R* and *S*,*S* **Bip** carrier ligands to platinum precursors results exclusively in the C_2-symmetrical

(9) Kozelka, J.; Fouchet, M.-H.; Chottard, J.-C. *Eur. J. Biochem.* **1992**, *205*, 895−906.
(10) Cramer, R. E.; Dahlstrom, P. L. *J. Am. Chem. Soc.* **1979**, *101*, 3679−3681.
(11) Xu, Y.; Natile, G.; Intini, F. P.; Marzilli, L. G. *J. Am. Chem. Soc.* **1990**, *112*, 8177−8179.
(12) Dijt, F. J.; Canters, G. W.; den Hartog, J. H. J.; Marcelis, A. T. M.; Reedijk, J. *J. Am. Chem. Soc.* **1984**, *106*, 3644−3647.
(13) Ano, S. O.; Intini, F. P.; Natile, G.; Marzilli, L. G. *Inorg. Chem.* **1999**, *38*, 2989−2999.
(14) Buckingham, D. A.; Marzilli, L. G.; Sargeson, A. M. *J. Am. Chem. Soc.* **1969**, *91*, 5227−5232.
(15) Cerasino, L.; Williams, K. M.; Intini, F. P.; Cini, R.; Marzilli, L. G.; Natile, G. *Inorg. Chem.* **1997**, *36*, 6070−6079.

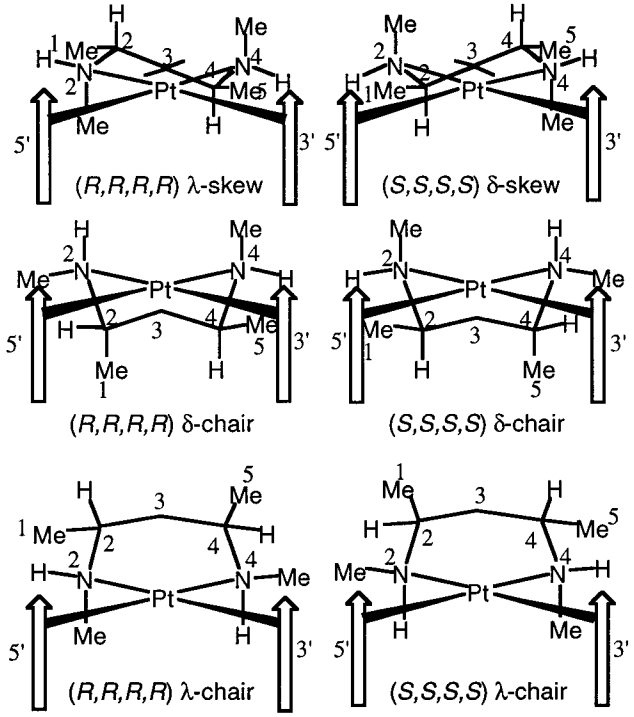

Figure 3. Isomers of (*R*,*R*,*R*,*R*)- and (*S*,*S*,*S*,*S*)-**Me$_2$DAP**Pt(GpG) in which GpG is in the HH1 conformation and **Me$_2$DAP** is in the three favored conformations. For clarity, the phosphodiester backbone is not shown.

S,*R*,*R*,*S* and *R*,*S*,*S*,*R* configurations, respectively.[3] This feature, which results from the tying of the asymmetric nitrogens within the piperidine rings, overcomes the problem of multiple isomers. Retromodels with **Bip** are also among the most informative models because the ligand possesses in-plane bulk that results in about a billion-fold decrease in the rate of rotation around the Pt−N7 bond.[16] We have recently established that variants in non-HH1 conformer classes are possible for **Bip**Pt(GpG) and **Bip**Pt(d(GpG)).[3−5,16] The stereochemistry of the **Bip** carrier ligand influences the conformer distribution and controls cross-link handedness; thus, **Bip** is an example of a chirality-controlling chelate (CCC) ligand. (*S*,*R*,*R*,*S*)-**Bip**Pt(d(GpG)) and (*S*,*R*,*R*,*S*)-**Bip**Pt(GpG) both favored two variants, *anti*, *anti* HH1 L and *anti*, *syn* ΔHT1 L.[4,5] When these complexes were kept at pH 10 for several days, the ΔHT1 L variant became favored over the HH1 L variant, demonstrating that ΔHT1 L is more favorable when N1 is deprotonated.[5,16] The two conformers of (*R*,*S*,*S*,*R*)-**Bip**Pt(d(GpG)) at physiological pH were *anti*, *anti* HH1 R and *anti*, *anti* HH2 R (Figure 1).[3] A later study of (*R*,*S*,*S*,*R*)-**Bip**Pt(d(GpG)) showed that the ΛHT2 R conformer (Figure 1) becomes ∼30% abundant when the sample is kept for 1 day at pH 10, where N1 is not protonated.[16] Furthermore, signals appeared at high pH that did not disappear at low pH; these signals were assigned to a product in which the **Bip** ligand had isomerized. Interestingly, no HH2 R variant was observed for (*R*,*S*,*S*,*R*)-**Bip**Pt(GpG) at any pH, and only a small population of ΛHT2 R was observed at pH 10;[5] these results suggested that fewer abundant conformers are present in *cis*-PtA$_2$(GpG) complexes than in *cis*-PtA$_2$(d(GpG)) complexes.

These studies established an interplay between the carrier ligand influencing d(GpG) or GpG conformation and the d(GpG) or GpG influencing carrier ligand configuration. The latter influence cannot be assessed easily with the **Bip** ligand because the *R*,*S*,*S*,*S* and *S*,*R*,*R*,*R* stereochemistries are not favorable, and starting complexes with these stereochemistries cannot be studied. However, complexes with the **Me$_2$DAP** ligand are available in sufficient quantity except for those with the *S*,*R*,*R*,*S* and *R*,*S*,*S*,*R* configurations.[15] The *S*,*R*,*R*,*R* and *S*,*S*,*S*,*R* configurations are non-C_2-symmetrical, and thus, two linkage isomers result for both (*S*,*R*,*R*,*R*)- and (*S*,*S*,*S*,*R*)-**Me$_2$DAP**Pt(GpG). We will use the designations 5′-*cis*-*S* and 5′-*cis*-*R* for the linkage isomers with the 5′-G base *cis* to the *S* and *R* nitrogens, respectively. For these complexes, we number the **Me$_2$DAP** atoms starting from the C−Me group near the end with the *S* nitrogen (Figure 2). For the (*R*,*R*,*R*,*R*)- and (*S*,*S*,*S*,*S*)-**Me$_2$DAP**Pt(GpG) adducts, the **Me$_2$DAP** ligands lose C_2 symmetry; thus, we have arbitrarily chosen to begin numbering the coordinated ligand starting from the end that is *cis* to the 5′-G base (Figure 3). We shall use a superscript to designate the atom number.

For each **Me$_2$DAP** configuration, the six-membered chelate ring can assume both skew and chair conformations (Figures 2 and 3). The two most likely skew conformations have the three ring carbons and the platinum atom coplanar; these skew conformations have a true helicity of the ring pucker. The puckers are designated δ and λ; when the complexes are viewed from the **Me$_2$DAP** side of the coordination plane, a line connecting two atoms of the carbon chain will be rotated (by an angle less than 90°) clockwise (λ) or counterclockwise (δ) to be aligned with the platinum coordination plane (Figures 2 and 3). Two chair conformations are possible; these do not possess a true helicity, and therefore, a pseudohelicity is designated by choosing the C^2-C^3 bond. For **Me$_2$DAP**PtCl$_2$ complexes,[15] the favored conformation for the *S*,*R*,*R*,*R* and *S*,*S*,*S*,*R* stereochemistries was δ chair. For the *R*,*R*,*R*,*R* stereochemistry a mixture of both chair conformations and the λ-skew conformation existed, and for the *S*,*S*,*S*,*S* stereochemistry the favored conformations were the two chair conformations and the δ-skew conformation.

In general, the N−Me groups of the coordinated **Me$_2$DAP** ligand favor axial positions over equatorial positions.[15,17] Furthermore, many of the favored conformations of the **Me$_2$DAP** ligands have one C−Me group in an axial position. Thus, the **Me$_2$DAP** complexes typically possess carrier ligand bulk that is significantly out of the coordination plane. Such bulk could affect the GpG ligand conformations by disfavoring certain variants due to steric interligand clashes.

In **Me$_2$DAP**Pt**G**$_2$ complexes, axial N−Me groups were calculated to affect the barrier to **G** base rotation only slightly; thus, for each **Me$_2$DAP**Pt**G**$_2$ complex at room temperature, only one set of NMR resonances was observed.[17] Accordingly, we hoped that **Me$_2$DAP**Pt(GpG) adducts would have dynamic properties between those of *cis*-Pt(NH$_3$)$_2$(GpG) and **Bip**Pt(GpG) adducts.[16] If rotation around the Pt−N7 bond is slowed by the presence of a phosphodiester linkage relative to **Me$_2$DAP**Pt**G**$_2$, we might detect atropisomers for **Me$_2$DAP**Pt(GpG).

Previously we found that [**Me$_2$DAP**Pt(9-EtG)$_2$]$^{2+}$ complexes [9-EtG = 9-ethylguanine] isomerize at the nitrogen centers at high pH; on isomerization at pH 10 the [(*R*,*R*,*R*,*R*)-**Me$_2$DAP**Pt(9-EtG)$_2$]$^{2+}$ complex gave a 4:2:1 distribution of *S*,*R*,*R*,*R*/*R*,*R*,*R*,*R*/*S*,*R*,*R*,*S* carrier ligand configurations.[17] However, when a chiral ligand such as GpG replaces the two 9-EtG ligands, we expect that the distribution will be different. We examined the carrier ligand distribution for the **Me$_2$DAP**Pt(GpG) complexes in order to understand better the interligand interactions in these complexes. Furthermore, we wanted to study how non-

(16) Williams, K. M.; Cerasino, L.; Natile, G.; Marzilli, L. G. Manuscript in preparation.

(17) Williams, K. M.; Cerasino, L.; Intini, F. P.; Natile, G.; Marzilli, L. G. *Inorg. Chem.* **1998**, *37*, 5260−5268.

C_2-symmetrical carrier ligands affect the distribution of the different GpG variants.

Materials and Methods

GpG (Et_3NH^+ salt, Aldrich) was used as received. The preparation and characterization of **Me$_2$DAP**$PtCl_2$ complexes has been described previously.[15]

Me$_2$DAPPt(GpG). (*R*,*R*,*R*,*R*)-, (*S*,*R*,*R*,*R*)-, (*S*,*S*,*S*,*R*)-, or (*S*,*S*,*S*,*S*)-**Me$_2$DAP**$PtCl_2$ (~2.5 μmol) was added to D_2O (2.0 mL). GpG (~2.5 μmol) in D_2O (1.5 mL) was added to each solution, and the pH (uncorrected) was adjusted to ~4.5. Samples were typically kept at room temperature, although samples kept in an ice bath were found to have similar product distributions. After an aliquot of each sample was checked by NMR spectroscopy to confirm that the reaction was complete, the sample was transferred to an NMR tube and dried by blowing air onto the sample. After drying, the sample was dissolved in 600 μL of D_2O.

NMR Spectroscopy. NMR spectra were collected on a GE Omega GN-600 spectrometer as described recently.[5] In our studies of retro models of this general size, we have not found differences in relative cross-peak intensities in nuclear Overhauser effect spectroscopy (NOESY) and rotating-frame Overhauser enhancement spectroscopy (ROESY). NOESY spectra are employed here because the cross-peaks were larger relative to the noise. Unless otherwise indicated, the spectra were collected at room temperature in D_2O. Spectra were referenced to the residual HOD signal (^{1}H) or TMP (^{31}P).

CD Spectroscopy. CD spectra of **Me$_2$DAP**Pt(GpG) samples (40−50 μM in 0.1 M NaCl) were acquired from 200 to 400 nm on a Jasco J-600 spectropolarimeter at room temperature.

Molecular Modeling. MMD calculations were performed on a Silicon Graphics INDY R5000 workstation using the InsightII package, version 97.0 (MSI). A modified version of the AMBER force field was employed; charges and potential types were set using methods described previously.[18] Different conformations of the **Me$_2$DAP** ligand were generated by using dynamics to simulate heating at 1800 K for 250 ps while keeping the coordinates of the GpG ligand fixed; these structures were then minimized with the GpG ligand fixed in order to determine the low-energy **Me$_2$DAP** ligand conformations (Supporting Information). The fixed GpG coordinates were obtained by an initial minimization to obtain conformations lacking clashes and similar to those found previously.[5] For each low-energy conformation of the **Me$_2$DAP** ligand, dynamics at 300 K for 250 ps generated 250 structures that were fully minimized.

Results

(*R*,*R*,*R*,*R*)-Me$_2$DAPPt(GpG). After a solution of GpG and (*R*,*R*,*R*,*R*)-**Me$_2$DAP**$PtCl_2$ at pH ~4.5 was prepared as above, new resonances began to appear after ~1.5 h (Supporting Information). After 1 day, the reaction was complete. Two H8 NMR peaks at 8.78 and 8.47 ppm observed at 5 °C at pH 4.5 (Figure 4) were assigned to 5′-G H8 and 3′-G H8 of (*R*,*R*,*R*,*R*)-**Me$_2$DAP**Pt(GpG), respectively, as will be discussed below; these peaks had line widths of 8 and 7 Hz, respectively. Likewise, only one set of relatively sharp **Me$_2$DAP** signals was observed (Supporting Information). The presence of only one set of NMR signals is consistent with either one dominant form or with multiple forms in fast exchange (i.e., the dynamic motion problem). When the (*R*,*R*,*R*,*R*)-**Me$_2$DAP**Pt(GpG) sample was warmed to 40 °C, the **Me$_2$DAP** signals (Supporting Information) and the 3′-G H8 signal remained sharp while the 5′-G H8 signal broadened to ~20 Hz (Figure 4), suggesting moderately fast exchange with a second GpG form at 40 °C. When the sample was placed in 2:1 CD_3OD/D_2O, the H8 signals shifted slightly downfield to 8.88 and 8.51 ppm and had line widths of 10 and 5 Hz, respectively, at room temperature. When this sample was cooled to −40 °C (Figure 4), the H8 signals broadened slightly (11 and 9 Hz, respectively) and shifted slightly (8.85 and 8.67 ppm, respectively). This lack of significant broadening of the H8 signals suggests that the GpG exists as only one major form at −40 °C. The broadness of the **Me$_2$DAP** signals at −40 °C (Supporting Information) suggests moderate exchange of the **Me$_2$DAP** ligand. The ^{31}P NMR spectrum of (*R*,*R*,*R*,*R*)-**Me$_2$DAP**Pt(GpG) at pH 4.5 at room temperature had one signal (Figure 5, Table 1). The −3.31 ppm shift is almost identical to that of the *anti*, *anti* HH1 R variant (−3.32 ppm) of (*R*,*S*,*S*,*R*)-**Bip**Pt(GpG).[5]

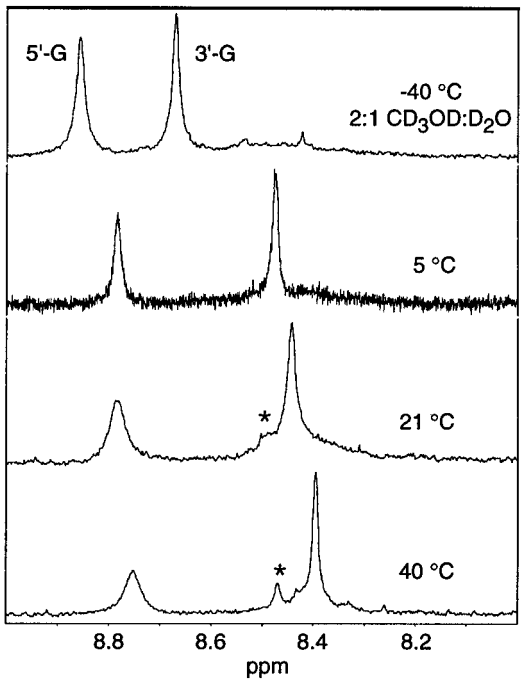

Figure 4. H8 region of the ^{1}H NMR spectrum of (*R*,*R*,*R*,*R*)-**Me$_2$DAP**Pt(GpG) at various temperatures: (top to bottom) −40 °C in 2:1 CD_3OD/D_2O and 5, 21, and 40 °C in D_2O. The small peak at ~8.46 ppm (marked with an asterisk in the bottom two spectra) is an impurity.

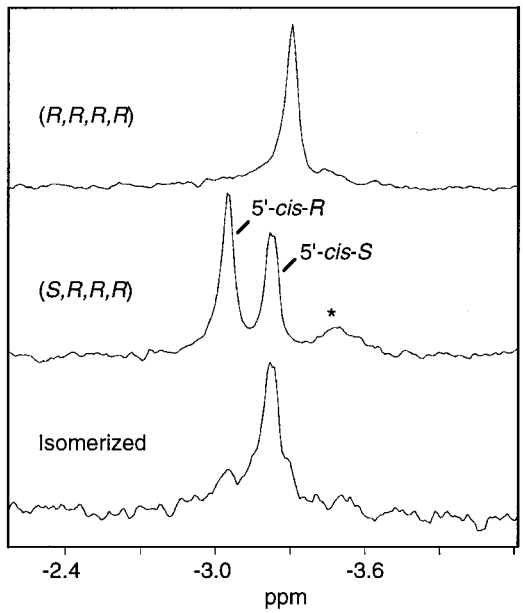

Figure 5. Room temperature ^{31}P NMR spectra of (*R*,*R*,*R*,*R*)-**Me$_2$DAP**Pt(GpG) (top), (*S*,*R*,*R*,*R*)-**Me$_2$DAP**Pt(GpG) (middle), and a sample of (*S*,*R*,*R*,*R*)-**Me$_2$DAP**Pt(GpG) that had been isomerized at about pH 10 (bottom). All spectra were collected at about pH 4.5. The peak designated by an asterisk in the middle spectrum is thought to be an impurity.

Table 1. ^{1}H and ^{31}P NMR Assignments (ppm) for GpG in *cis*-PtA_2(GpG) Complexes[a]

		G	H8	H1′	H2′	H3′	H4′	^{31}P
(*S,R,R,S*)-**Bip**Pt(GpG)	HH1 L	5′	8.10	5.86	4.22	4.90	4.25	−3.17
		3′	9.10	5.90	4.72	4.47	4.32	
	ΔHT1 L	5′	7.84	5.92	4.51	3.84	4.18	−4.78
		3′	7.96	5.68	5.21	4.88	4.14	
(*R,S,S,R*)-**Bip**Pt(GpG)	HH1 R	5′	8.78	6.09	4.23	4.70	4.39	−3.32
		3′	8.10	5.88	4.24	4.30	4.27	
cis-$Pt(NH_3)_2$(GpG)		5′	8.54	6.02	4.34	4.56	4.31	−3.64
		3′	8.31	5.87	4.53	4.42	4.28	
(*R,R,R,R*)-**Me$_2$DAP**Pt(GpG)		5′	8.78	6.06	4.15	4.74	4.33	−3.31
		3′	8.47	5.85	4.34	4.34	4.26	
(*S,R,R,R*)-**Me$_2$DAP**Pt(GpG)		5′	8.94	6.10	4.11	4.80	4.36	−3.23
5′-*cis*-*S* linkage isomer		3′	8.34	5.88	4.33	4.12	4.28	
(*S,R,R,R*)-**Me$_2$DAP**Pt(GpG)		5′	8.43	5.96	4.16	4.58	*b*	−3.05
5′-*cis*-*R* linkage isomer		3′	8.70	5.90	4.47	*b*	*b*	

[a] Spectra collected at about pH 4 at 5 °C in D_2O. ^{31}P NMR shifts measured at room temperature. [b] Signals could not be assigned.

Table 2. Me$_2$DAP Ligand ^{1}H NMR Signals (ppm) for **Me$_2$DAP**Pt(GpG) Complexes

Me$_2$DAP configuration		$N^{2,4}H$	$N^{2,4}Me$	$C^{2,4}H$	$C^{2,4}Me$	C^3H_2[a]
(*R,R,R,R*)-**Me$_2$DAP**	*cis* to 5′-G	5.93	2.26	3.21	1.56	2.02
	cis to 3′-G	5.76	2.43	3.95	1.28	1.89
(*S,R,R,R*)-**Me$_2$DAP**	*cis* to 5′-G	6.21	2.78	2.67	1.64	1.60
5′-*cis*-*S* linkage isomer	*cis* to 3′-G	5.67	2.56	4.12	1.17	2.35

[a] Methylene signals not distinguished.

Assignment of the ^{1}H NMR signals of (*R,R,R,R*)-**Me$_2$DAP**Pt(GpG) at 5 °C in D_2O was possible from NOESY and COSY spectra (Table S1 of Supporting Information). The $^3J_{H1'-H2'}$ value of 7.5 Hz indicated that the 3′ sugar was primarily S. An H8−H8 NOE cross-peak indicated that the bases are primarily in an HH orientation (Supporting Information). The presence of moderately strong H8−H2′ and H8−H3′ NOE cross-peaks (Supporting Information) and the lack of H8−H1′ NOE cross-peaks indicated that both nucleotides are primarily *anti*. With the exception of the 3′-G H8 signal, all of the assigned GpG signals in the (*R,R,R,R*)-**Me$_2$DAP**Pt(GpG) complex were within 0.1 ppm of the corresponding signals of the (*R,S,S,R*)-**Bip**Pt(GpG) complex (Table 1). This result strongly suggests that the dominant variant of (*R,R,R,R*)-**Me$_2$DAP**Pt(GpG) is the *anti*, *anti* HH1 R variant. However, the 3′-G H8 signal of (*R,R,R,R*)-**Me$_2$DAP**Pt(GpG) complex is at 8.47 ppm compared to 8.10 ppm for the (*R,S,S,R*)-**Bip**Pt(GpG) complex, indicating that the 3′-G base is not so canted in the **Me$_2$DAP** complex.

The **Me$_2$DAP** signals of this complex were also assigned (Table 2 and Supporting Information). An NOE cross-peak from 5′-G H8 to the N^2Me group is unusual because 5′-G H8 and the N^2Me group are on opposite sides of the coordination plane when the GpG ligand is an HH1 conformer (Figure 3); however, structures from our MMD calculations (see below) indicated that these groups are within ∼3.5 Å when **Me$_2$DAP** is in the δ-chair conformation in which the N^2Me group is equatorial. The signal of N^2H (5.93 ppm) was downfield of the signal of N^4H (5.76 ppm), suggesting that the 3′-G O6 does not form a hydrogen bond to the **Me$_2$DAP** N^4H.

The CD spectrum of (*R,R,R,R*)-**Me$_2$DAP**Pt(GpG) at pH 4.5 has two strong positive features at ∼290 and ∼270 nm, a slightly weaker positive feature at ∼230 nm, and a strong negative feature at ∼210 nm (Figure 6). The intensities of these features are unusually strong for an HH conformer, and this CD spectrum is unlike that of any **Bip**Pt(GpG) variant at low pH.[5]

MMD calculations were performed on the (*R,R,R,R*)-**Me$_2$DAP**Pt(GpG) complex with the GpG geometry fixed in the *anti*, *anti* HH1 R conformation. The three lowest energy conformations computed for the **Me$_2$DAP** ligand were δ chair, λ chair, and λ skew (Supporting Information). Similarly, these three conformations were predicted to be the lowest in energy for both (*R,R,R,R*)-**Me$_2$DAP**$PtCl_2$[15] and [(*R,R,R,R*)-**Me$_2$DAP**Pt(9-EtG)$_2$]$^{2+}$,[17] and NMR methods confirmed that the **Me$_2$DAP** was fluxional for these complexes. In fully minimized structures of (*R,R,R,R*)-**Me$_2$DAP**Pt(GpG) with GpG in an *anti*, *anti* HH1 conformation, the lowest energy structure with the λ-skew conformation was ∼2 kcal/mol more stable than the lowest energy structures with the chair conformations (Table 3); the major contribution to this extra stability was a 3′-G O6 to **Me$_2$DAP** N^4H hydrogen bond, which resulted in significant canting of the 3′-G (i.e., R canting) in this calculated structure (Figure 7). The 3′-G was canted to a lesser extent in the δ-chair conformer and uncanted in the λ-chair conformer (Figure 7).

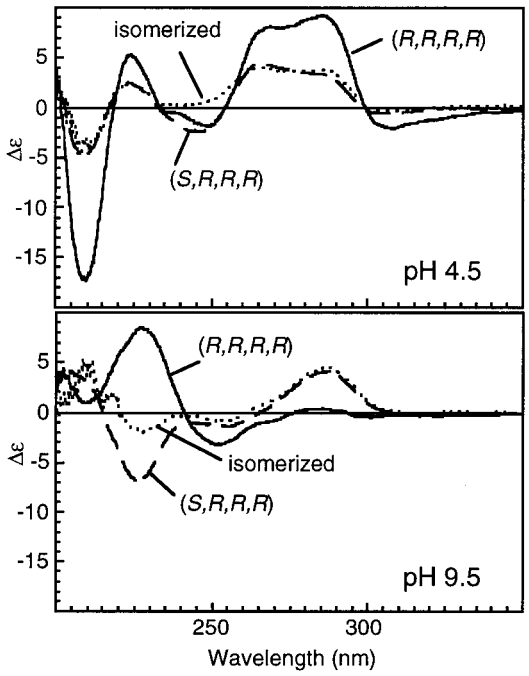

Figure 6. CD spectra of (*R,R,R,R*)-**Me$_2$DAP**Pt(GpG) (solid line), (*S,R,R,R*)-**Me$_2$DAP**Pt(GpG) (dashed line), and the isomerized (*R,R,R,R*)-**Me$_2$DAP**Pt(GpG) sample (dotted line) at pH 4.5 (top) and 9.5 (bottom).

(*S,R,R,R*)-Me$_2$DAPPt(GpG). When GpG was added to a solution of (*S,R,R,R*)-**Me$_2$DAP**$PtCl_2$, new resonances appeared after a few hours (Supporting Information). After 1 day, four H8 NMR signals of comparable intensity were observed (Figure 8). Because the (*S,R,R,R*)-**Me$_2$DAP** ligand is non-C_2-symmetrical, two linkage isomers of (*S,R,R,R*)-**Me$_2$DAP**Pt(GpG),

Table 3. Energies of Fully Minimized **Me$_2$DAP**Pt(GpG) MMD Structures[a]

Me$_2$DAP configuration	linkage isomer	**Me$_2$DAP** conformation	GpG variant	*cis*-N−Pt−N7−C5 torsion angle (deg)[b] 5′-G	3′-G	energy (kcal/mol)
S,R,R,R	5′-*cis*-*S*	δ chair	*anti*, *anti* HH1 R	98	−74	8.68[c]
S,R,R,R	5′-*cis*-*R*	δ chair	*anti*, *anti* HH1	93	−89	10.67[c]
R,R,R,R		δ chair	*anti*, *anti* HH1 R	94	−78	9.82[c]
		λ chair	*anti*, *anti* HH1	88	−92	10.01[c]
		λ skew	*anti*, *anti* HH1 R	106	−62	7.72[d]
S,S,S,R	5′-*cis*-*S*	δ chair	*anti*, *anti* HH1 L	69	−102	7.66[d]
			anti, *syn* ΔHT1 L	73	93	9.48[c]
S,S,S,R	5′-*cis*-*R*	δ chair	*anti*, *anti* HH1	91	−93	10.20[c]
			anti, *syn* ΔHT1 L	92	79	6.47
S,S,S,S		δ chair	*anti*, *anti* HH1	76	−99	9.66
			anti, *syn* ΔHT1 L	81	88	6.82
		δ skew	*anti*, *anti* HH1 L	64	−105	6.45[d]
			anti, *syn* ΔHT1 L	62	83	4.84[d]
		λ chair	*anti*, *anti* HH1 L	99	−85	8.42
			anti, *syn* ΔHT1 L	89	82	6.74

[a] Only structures with **Me$_2$DAP** conformations that were predicted to be energetically favorable are listed. [b] Torsion angle is defined as 0° when the G base is coplanar with the platinum coordination plane with H8 pointing toward other G. Positive values indicate a counterclockwise rotation when viewing from the nucleotide side of the coordination plane. [c] 5′-G 2′-OH−phosphate group hydrogen bond. [d] G O6−**Me$_2$DAP** NH hydrogen bond.

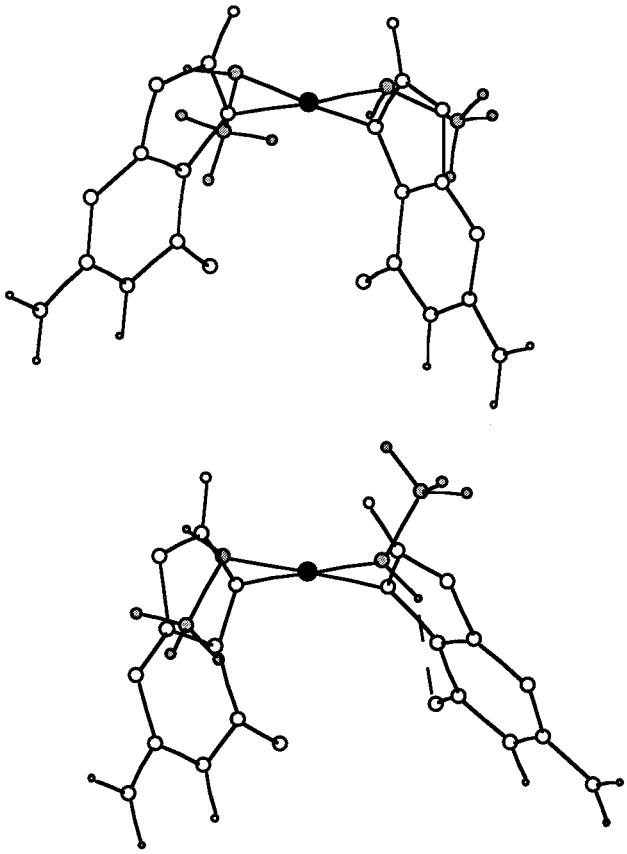

Figure 7. Lowest-energy MMD calculated structures of (*R,R,R,R*)-**Me$_2$DAP**Pt(GpG) with the carrier ligand in the λ-chair (top) and λ-skew (bottom) conformations, showing the backbone. For clarity, only the G bases and the relevant portions of **Me$_2$DAP** are shown. Dashed line indicates the 3′-G O6 to N^{4}H hydrogen bond in the bottom structure.

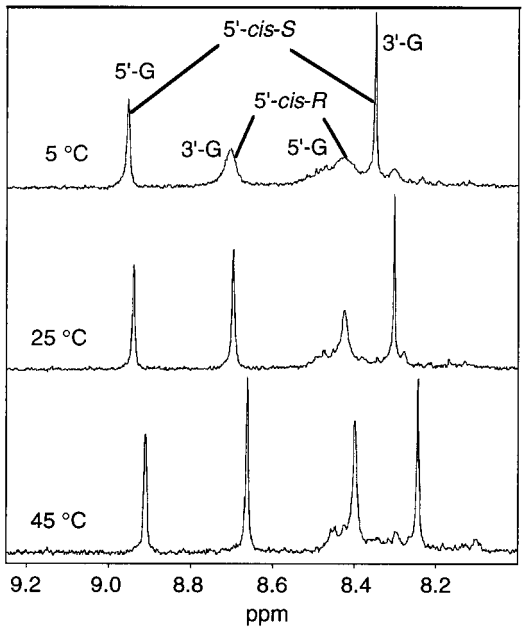

Figure 8. H8 region of the ^{1}H NMR spectrum of (*S,R,R,R*)-**Me$_2$DAP**Pt(GpG) at pH 5 in D_2O at 5 °C (top), 25 °C (middle), and 45 °C (bottom).

designated as 5′-*cis*-*S* and 5′-*cis*-*R*, are possible (Figure 2). The presence of two pairs of resonances of similar intensities indicates that both linkage isomers of (*S,R,R,R*)-**Me$_2$DAP**Pt(GpG) are kinetically favorable. Thus, the rate of formation of the Pt−N7 bond is not controlled by the stereochemistry of the *cis* nitrogen.

The H8 signals of the 5′-*cis*-*S* linkage isomer [5′-G H8 (8.94 ppm) and 3′-G H8 (8.30 ppm)] were both sharp (∼2−3 Hz) at room temperature; the **Me$_2$DAP** signals were also sharp (typically less than 5 Hz). Thus, either one conformer dominates or several conformers exist, and exchange between these conformers is very fast. The line widths of the NMR signals remained sharp when the temperature was lowered to 5 °C (Figure 8). In contrast, the H8 signals of *cis*-Pt(NH$_3$)$_2$(GpG) and *cis*-Pt(NH$_3$)$_2$(d(GpG)) broadened as the temperature was lowered to 5 °C, and this behavior was attributed to slowing exchange between conformers.[5,16] The lack of such broadening for the H8 signals of this isomer of (*S,R,R,R*)-**Me$_2$DAP**Pt(GpG) indicates that it has one dominant conformer.

The 5′-G H1′ of (*S,R,R,R*)-**Me$_2$DAP**Pt(GpG) was a singlet, indicating an N conformation; N7−Pt−N7 cross-links are known to have an N conformer for the 5′ sugar.[3,5,8,16] The presence of H8−H2′ and H8−H3′ NOE cross-peaks (Supporting Information) and the absence of H8−H1′ NOE cross-peaks indicated that the G residues were mostly *anti*. A weak H8−H8 NOE cross-peak (Supporting Information) and the relatively large shift difference of the H8 signals (Table 1) indicated that

the GpG in this isomer had primarily an HH conformation. The 3′-G H8 signal is upfield of the 5′-G H8 signal, indicating that the major conformer is either *anti*, *anti* HH1 R or *anti*, *anti* HH2 L (Figure 1). However, no HH2 conformer was formed in **Bip**Pt(GpG) complexes, and thus, HH2 is unlikely to be a dominant form.[5] Furthermore, L canting was not observed for any minimum-energy structures of (*S*,*R*,*R*,*R*)-**Me$_2$DAP**Pt(GpG) conformers (Supporting Information). Thus, the dominant conformation is *anti*, *anti* HH1 R.

For the 5′-*cis*-*R* (*S*,*R*,*R*,*R*)-**Me$_2$DAP**Pt(GpG) linkage isomer at 5 °C, a weak NOE cross-peak from 5′-G H1′ to a signal at 4.16 ppm assigned this signal to 5′-G H2′. A weak H8−H8 NOE cross-peak indicated a significant population of an HH conformation. The presence of H8−H2′ or H8−H3′ NOE cross-peaks and the lack of H8−H1′ NOE cross-peaks indicated that the G's were mostly *anti*.

(*S*,*R*,*R*,*R*)-**Me$_2$DAP**Pt(GpG) at pH 4.5 had ^{31}P NMR signals at −3.23 and −3.05 ppm at room temperature (Figure 5, Table 1) assigned to the 5′-*cis*-*S* and 5′-*cis*-*R* isomers, respectively, as explained below. These ^{31}P NMR shifts are very similar to those found for the HH1 conformers of **Bip**Pt(GpG) complexes (−3.17 and −3.32 ppm for HH1 L and HH1 R, respectively).[5]

The CD spectrum of (*S*,*R*,*R*,*R*)-**Me$_2$DAP**Pt(GpG) was collected at pH 4.5 (Figure 6). The pH was then raised to 9.5 and a spectrum recorded immediately (Figure 6). These initial spectra were very similar to those of (*R*,*S*,*S*,*R*)-**Bip**Pt(GpG),[5] suggesting that the HH1 R variant is favored for both linkage isomers of (*S*,*R*,*R*,*R*)-**Me$_2$DAP**Pt(GpG). As discussed later, isomerization of the **Me$_2$DAP** ligand occurs with time at high pH (Figure 6).

The carrier ligand in the lowest energy structures calculated previously for the (*S*,*R*,*R*,*R*)-**Me$_2$DAP**PtCl$_2$[15] and [(*S*,*R*,*R*,*R*)-**Me$_2$DAP**Pt(9-EtG)$_2$]$^{2+}$ [17] compounds had the *δ*-chair conformation; this conformation was confirmed for both complexes by NMR methods. MMD calculations on both (*S*,*R*,*R*,*R*)-**Me$_2$DAP**Pt(GpG) linkage isomers with the GpG ligand fixed in an HH1 conformation indicated that the **Me$_2$DAP** ligand also strongly favors the *δ*-chair conformation, which has both N−Me groups in the axial positions (Figure 2), by ∼4 kcal/mol (Supporting Information). For the 5′-*cis*-*S* isomer, the 3′-G base was canted, but no amine−O6 hydrogen bond was formed (Table 3). The lowest energy structure of the 5′-*cis*-*R* HH1 conformer, which was calculated to be 2 kcal/mol less stable than that of the corresponding 5′-*cis*-*S* conformer, had no notable canting (Table 3).

(*S*,*S*,*S*,*S*)-Me$_2$DAPPt(GpG). The ^{1}H NMR spectrum of (*S*,*S*,*S*,*S*)-**Me$_2$DAP**Pt(GpG) at pH 4.5 at 21 °C had a very broad feature at ∼8.0 ppm and a cluster of small, sharp signals in the 8.3−8.4 ppm range (Figure 9). At 5 °C, the broad feature was resolved into two features (Figure 9) with H8 shifts similar to those of the *anti*, *syn* ΔHT1 L variant of (*S*,*R*,*R*,*S*)-**Bip**Pt(GpG). These observations indicate that (*S*,*S*,*S*,*S*)-**Me$_2$DAP**Pt(GpG) exists as a mixture of conformers in moderate exchange at 21 °C, and the upfield H8 shifts suggest that ΔHT1 L is a major conformer.

The ^{31}P NMR spectrum of (*S*,*S*,*S*,*S*)-**Me$_2$DAP**Pt(GpG) has a very broad signal at ca. −4.8 ppm and a somewhat sharper signal at −3.47 ppm. The two signals are of approximately equal intensity, suggesting that two major forms are present in ∼50% abundance. Since the ^{31}P NMR signal of the *anti*, *syn* ΔHT1 L variant of (*S*,*R*,*R*,*S*)-**Bip**Pt(GpG) is at −4.78 ppm,[5] we suggest that the signal at −4.8 ppm is due to a ΔHT1 conformer. The signal at −3.47 ppm is only slightly upfield from the −3.1 to −3.3 ppm range that has been observed for HH1 conformers,

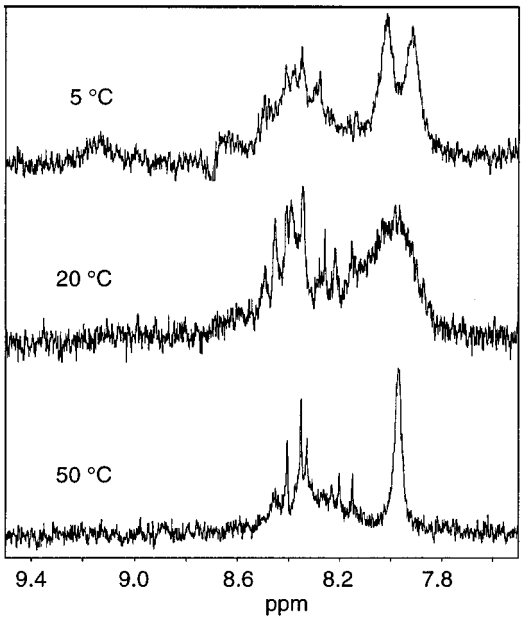

Figure 9. H8 region of the ^{1}H NMR spectrum of (*S*,*S*,*S*,*S*)-**Me$_2$DAP**Pt(GpG) at pH 5 at 5 °C (top), 20 °C (middle), and 50 °C (bottom).

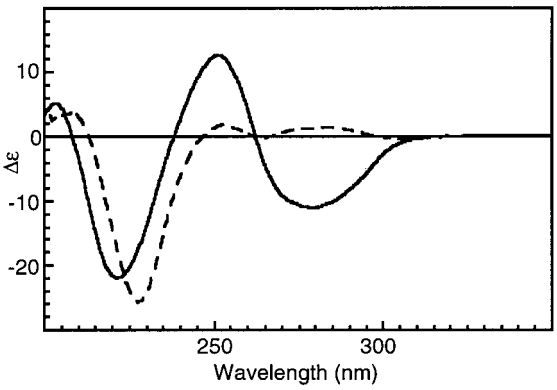

Figure 10. CD spectra of (*S*,*S*,*S*,*S*)-**Me$_2$DAP**Pt(GpG) at pH 5 (solid line) and pH 9.4 (dashed line).

suggesting that the −3.47 ppm signal might belong to an HH1 conformer.[5]

MMD calculations with the GpG fixed in either the HH1 or the ΔHT1 conformer suggested that the lowest energy conformations of the **Me$_2$DAP** ligand of (*S*,*S*,*S*,*S*)-**Me$_2$DAP**Pt(GpG) were the *δ*-chair, *λ*-chair, and *δ*-skew conformations (Supporting Information). For each **Me$_2$DAP** conformation, the ΔHT1 conformer was calculated to be slightly lower in energy than the HH1 conformer (Table 3). Two **Me$_2$DAP** NH−G O6 hydrogen bonds appear to be possible for the ΔHT1 conformer with the **Me$_2$DAP** in the *δ*-skew conformation. However, only the 5′-G O6 had such a hydrogen bond in the energy-minimized structures.

The CD spectrum of (*S*,*S*,*S*,*S*)-**Me$_2$DAP**Pt(GpG) at pH 5 has strong negative features at 280 and 220 nm and a strong positive feature at 250 nm (Figure 10); this type of spectrum is characteristic of a ΔHT chirality for both *cis*-PtA$_2$**G**$_2$[17,20,21] and

(18) Yao, S. J.; Plastaras, J. P.; Marzilli, L. G. *Inorg. Chem.* **1994**, *33*, 6061−6077.
(19) Wüthrich, K. *NMR of Proteins and Nucleic Acids*; John Wiley & Sons: New York, 1986.
(20) Wong, H. C.; Intini, F. P.; Natile, G.; Marzilli, L. G. *Inorg. Chem.* **1999**, *38*, 1006−1014.
(21) Marzilli, L. G.; Intini, F. P.; Kiser, D.; Wong, H. C.; Ano, S. O.; Marzilli, P. A.; Natile, G. *Inorg. Chem.* **1998**, *37*, 6898−6905.

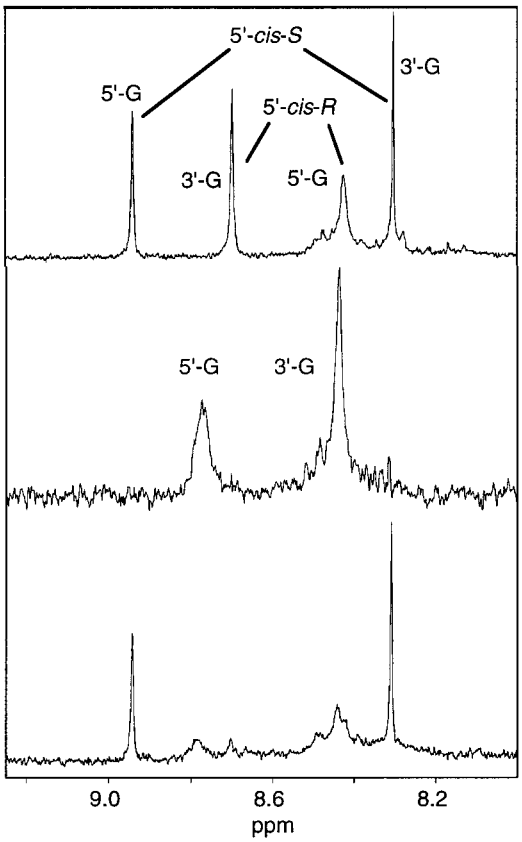

Figure 11. H8 regions of the room temperature ^{1}H NMR spectra of (*S,R,R,R*)-**Me$_2$DAP**Pt(GpG) (top) and (*R,R,R,R*)-**Me$_2$DAP**Pt(GpG) at pH 4.5 before (middle) and after (bottom) isomerization at pH 9.4.

cis-PtA_2(GpG)[5,16] complexes. As the pH was raised to 9.4, a strong negative feature at 230 nm and weak positive features at 250 and 280 nm were observed; similar features were observed in the deconvoluted CD spectrum of the *anti*, *syn* ΔHT1 L variant of (*S,R,R,S*)-**Bip**Pt(GpG) at pH 10.[5] These spectra indicate that (*S,S,S,S*)-**Me$_2$DAP**Pt(GpG) strongly favors the ΔHT1 conformation at both low and high pH.

(*S,S,S,R*)-Me$_2$DAPPt(GpG). (*S,S,S,R*)-**Me$_2$DAP**Pt(GpG) has four major H8 signals, one relatively sharp signal (∼8 Hz) at 8.28 ppm and three broad signals at 8.42, 8.12, and 7.93 ppm at 21 °C (Supporting Information). All four signals are relatively upfield, suggesting that a significant population of an HT form exists for both linkage isomers of (*S,S,S,R*)-**Me$_2$DAP**Pt(GpG). The CD spectrum of (*S,S,S,R*)-**Me$_2$DAP**Pt(GpG) at pH 5 has features indicative of a ΔHT1 conformer. MMD calculations on both linkage isomers with the GpG fixed in either the HH1 or the ΔHT1 conformation predicted that the lowest energy **Me$_2$DAP** conformation is *δ* chair (Table 3).

Isomerization of Me$_2$DAPPt(GpG). The pH of a sample of (*R,R,R,R*)-**Me$_2$DAP**Pt(GpG) was raised from 4.5 to 9.0, and the ^{1}H NMR spectrum was monitored over time (Supporting Information). Small new resonances began to appear within ∼1−2 h due to isomerization of the **Me$_2$DAP** ligand at high pH. After 2 days at pH 9.0 the isomerization reaction had reached equilibrium, so the pH was lowered to 4.5 and a spectrum was collected (Figure 11). We were unable to determine accurately the population of the isomers because some of the H8 signals were very broad while others were very sharp. However, the two major H8 peaks (at 8.94 and 8.31 ppm) corresponded to 5′-*cis-S* (*S,R,R,R*)-**Me$_2$DAP**Pt(GpG). The observation that one of the (*S,R,R,R*)-**Me$_2$DAP**Pt(GpG) linkage isomers is greatly favored over the other indicates that the GpG ligand is able to influence the configuration of the **Me$_2$DAP** ligand. The ^{31}P NMR spectrum of the isomerized sample had one major peak (at −3.23 ppm, Figure 5); thus, we can assign this peak to that of the 5′-*cis-S* linkage isomer of (*S,R,R,R*)-**Me$_2$DAP**Pt(GpG).

The pH of the (*R,R,R,R*)-**Me$_2$DAP**Pt(GpG) sample was raised to 9.5, and the CD spectrum recorded immediately had a weak negative feature at 250 nm and a stronger positive feature at 230 nm (Figure 6). After 2 h, these features had decreased in intensity and a weak positive feature appeared at 280 nm (Supporting Information). When the pH was dropped to 4.5 after 2 h at pH 9.5, the CD spectrum was much weaker in intensity than the original spectrum, and no changes occurred with time (Supporting Information). The observation of changes in the high pH CD spectrum that are irreversible at low pH indicated that partial isomerization of the nitrogen centers of the **Me$_2$DAP** ligand had occurred. The CD spectra of a fully isomerized sample at pH 4.5 and pH 9.5 were very similar to those of (*S,R,R,R*)-**Me$_2$DAP**Pt(GpG) (Figure 6). Thus, the CD and the NMR spectra were both useful for studying isomerization in the case of the carrier ligand isomers with the carbons having *R* chirality.

However, in the case of the carrier ligand isomers with the carbons having *S* chirality, CD spectroscopy was not a useful method for examining carrier ligand isomerization because the CD spectra of (*S,S,S,S*)-**Me$_2$DAP**Pt(GpG) and (*S,S,S,R*)-**Me$_2$DAP**Pt(GpG) are similar. When (*S,S,S,S*)-**Me$_2$DAP**Pt(GpG) was left at pH 9.4 for 2 h, very little change occurred in the CD spectrum; the feature at 280 nm became slightly weaker. A spectrum acquired immediately after the pH was lowered to 5 was nearly identical to the initial pH 5 spectrum. However, changes over time in the NMR spectrum of (*S,S,S,R*)-**Me$_2$DAP**Pt(GpG) at pH ∼9.6 did provide evidence for the isomerization of the **Me$_2$DAP** ligand. When the pH of (*S,S,S,R*)-**Me$_2$DAP**Pt(GpG) was raised to ∼9.6, new NMR resonances began to appear. After several days equilibrium was reached, and the pH of the sample was lowered to ∼4. The ^{1}H NMR spectrum at pH 4 (Supporting Information) contained resonances corresponding to (*S,S,S,S*)-**Me$_2$DAP**Pt(GpG); at least one linkage isomer of (*S,S,S,R*)-**Me$_2$DAP**Pt(GpG) was also present.

Discussion

Dynamic motion at a rate that could affect NMR line widths could occur either in the dinucleotide or in the carrier ligand of *cis*-PtA_2(GpG) and *cis*-PtA_2(d(GpG)) adducts. For **Bip**Pt(GpG) and **Bip**Pt(d(GpG)) complexes, conformational exchange requiring rotation of one or both G bases around the Pt−N7 bond was very slow relative to the NMR time scale;[3−5,16] thus, a different set of resonances could be observed for each conformer class. Within each conformer class, base wagging or rotation around the glycosyl bond leads to a number of possible variants; such exchange would likely be fast. The H8 signals of **Bip**Pt(GpG) and **Bip**Pt(d(GpG)) complexes were very sharp (2−3 Hz) at 5 °C; thus, if exchange between variants within a conformer class occurred, it was too fast to affect the line width of the signals. Sharp lines also require either that the **Bip** ligand is relatively rigid or that it undergoes rapid motion. The effect on the GpG and d(GpG) signals would be the same, but we believe that the ligand is relatively rigid.

In contrast, the *cis*-Pt$(NH_3)_2$ moiety is probably very dynamic, undergoing rapid rotation about the Pt−N single bonds. The H8 signals of *cis*-Pt$(NH_3)_2$(GpG) were relatively sharp (∼10 and 4 Hz for 5′-G H8 and 3′-G H8, respectively) at 21 °C but broader (∼20 and 5 Hz, respectively) at 5 °C.[5,16] Therefore,

exchange between conformer classes or between variants within a conformer class must be moderately fast at 21 °C and slower at 5 °C. Comparison to spectral data for **Bip**Pt(GpG) indicated that *cis*-Pt$(NH_3)_2$(GpG) exists as a mixture of variants from both the ΔHT1 and HH1 conformer classes;[5] thus, the most likely explanation for the broadening is exchange between conformer classes.

For many of the **Me$_2$DAP**Pt(GpG) isomers, broad H8 signals were observed, suggesting a dynamic process between those occurring in **Bip**Pt(GpG) and *cis*-Pt$(NH_3)_2$(GpG). Several lines of evidence exclude exchange between the **Me$_2$DAP** conformations as the cause of the broadening. For example, **Me$_2$DAP**PtCl_2 isomers have sharp **Me$_2$DAP** signals at room temperature, and broadening due to **Me$_2$DAP** conformational exchange was not observed above −50 °C for (*S*,*R*,*S*,*R*)-**Me$_2$DAP**PtCl_2.[15] Furthermore, the H8 resonances of (*S*,*R*,*S*,*R*)-**Me$_2$DAP**Pt(5′-GMP)$_2$ were sharp (<4 Hz) at both 25 and 5 °C even though exchange between **Me$_2$DAP** conformations was indicated by MMD calculations.[17] MMD calculations on [(*R*,*R*,*R*,*R*)-**Me$_2$DAP**Pt(9-EtG)$_2$]$^{2+}$ predicted that exchange between **Me$_2$DAP** conformations would have a lower energy barrier than rotation around the Pt−N7 bond.[17] The (*R*,*R*,*R*,*R*)-**Me$_2$DAP**Pt(d(GpG)) complex had very broad H8 signals (unpublished results) compared to those of the (*R*,*R*,*R*,*R*)-**Me$_2$DAP**Pt(GpG) analogue, suggesting that the differences in dynamic motion reside in the dinucleotide moiety. Finally, at −40 °C in 1:1 CD_3OD/D_2O, (*R*,*R*,*R*,*R*)-**Me$_2$DAP**Pt(GpG) has relatively sharp H8 signals (Figure 4) even though the **Me$_2$DAP** signals are broad (Supporting Information), suggesting that slowing of the dynamic motion of the **Me$_2$DAP** ligand does not significantly broaden the H8 signals. Therefore, all the evidence strongly indicates that the broadness of the H8 signals in the **Me$_2$DAP**Pt(GpG) complexes is due to dynamic motion within the GpG moiety. The broadness of the signals complicates the study of these complexes by 2D NMR methods; however, ^{31}P NMR and CD spectroscopies and MMD calculations can be utilized to supplement the ^{1}H NMR data in order to assess the conformations and properties of the adducts.

For the (*R*,*R*,*R*,*R*)-**Me$_2$DAP**Pt(GpG) complex, only one set of ^{1}H NMR resonances is observed (Table 1). The H8 resonances are relatively sharp (7−8 Hz) at 5 °C, but the 5′-G H8 signal is relatively broad (∼20 Hz) at 40 °C (Figure 4), suggesting that a second variant may become more favorable at high temperature. The shifts of the ^{1}H NMR signals at 5 °C are very similar to those of (*R*,*S*,*S*,*R*)-**Bip**Pt(GpG) (Table 1), suggesting that an *anti*, *anti* HH1 R variant dominates at this temperature. However, the 3′-G H8 signal is very downfield compared to the shift of the **Bip** analogue. MMD calculations suggest that the (*R*,*R*,*R*,*R*)-**Me$_2$DAP** ligand in reasonable *anti*, *anti* HH1 structures can have several conformations (Table 3). A hydrogen bond between 3′-G O6 and the **Me$_2$DAP** N^{4}H was predicted to be favorable only when the **Me$_2$DAP** is in the *λ*-skew conformation; the 3′-G base was canted ∼30° (*cis*-N−Pt−N7−C5 torsion angle of −62°, Table 3) in structures containing such a hydrogen bond. In MMD structures that did not have a hydrogen bond between 3′-G O6 and **Me$_2$DAP** N^{4}H, the 3′-G base was not very canted (Table 3). The 3′-G H8 signal is relatively downfield (Table 1), consistent with little canting. The relatively upfield shift of the N^{4}H signal (Table 2) also suggests that such a hydrogen bond does not form. Furthermore, the CD spectrum is unique (Figure 6), suggesting that this conformer might have some unusual features. Therefore, we conclude that (*R*,*R*,*R*,*R*)-**Me$_2$DAP**Pt(GpG) favors an *anti*, *anti* HH1 variant with a slight R canting.

(*S*,*R*,*R*,*R*)-**Me$_2$DAP**Pt(GpG) has two linkage isomers. Both are predicted from MMD calculations (Table 3) to have the **Me$_2$DAP** ligand in the *δ*-chair conformation, which has both N−Me groups axial (Figure 2). The one set of 5′-*cis*-*S* H8 signals observed has line widths (2−3 Hz) similar to those of **Bip**Pt(GpG) complexes.[5] The 5′-*cis*-*S* H8 signals remain sharp even at 5 °C (Figure 8), suggesting that one conformer is dominant. The ^{1}H NMR shifts of this isomer, with an upfield 3′-G H8 signal (Table 1, Figure 8), are very similar to those of (*R*,*S*,*S*,*R*)-**Bip**Pt(GpG),[5] for which the *anti*, *anti* HH1 R variant dominates. An HH1 conformer would be stable for 5′-*cis*-*S* (*S*,*R*,*R*,*R*)-**Me$_2$DAP**Pt(GpG) because there are no unfavorable interactions between the G O6 atoms and an N−Me or a C−Me group (Figure 2). Interestingly, the *anti*, *anti* HH1 R variant was predicted by MMD calculations to have no hydrogen bonds between 3′-G O6 and a **Me$_2$DAP** NH (Table 3). Furthermore, the signal of N^{4}H, which is *cis* to the 3′-G, is *upfield* of that of N^{2}H, which is *cis* to the 5′-G (Table 2). The opposite relationship of the **Me$_2$DAP** NH signals is expected if the 3′-G O6 formed a strong hydrogen bond to N^{4}H. Thus, steric factors and not hydrogen bonding appear to be the cause of the 3′-G canting.

For 5′-*cis*-*R* (*S*,*R*,*R*,*R*)-**Me$_2$DAP**Pt(GpG), the other linkage isomer, the H8 signals broadened as the temperature was lowered (Figure 8). Because MMD calculations predict that only the *δ*-chair conformation of the **Me$_2$DAP** ligand is favorable, moderately fast exchange between two or more GpG conformations is the most likely explanation for the broadening. Compared to cases with other carrier ligands and to the 5′-*cis*-*S* isomer, HH1 conformers should be somewhat unfavorable because the O6 atoms would be on the same side of the coordination plane as the N−Me groups (Figure 2). MMD calculations predicted that the 5′-*cis*-*R* *anti*, *anti* HH1 conformer would be 2 kcal/mol less stable than the corresponding 5′-*cis*-*S* conformer (Table 3). Thus, in addition to HH1, a second conformer is probably present.

HT conformers are known to have strong CD spectral features;[5,21] the lack of such characteristic features in the CD spectrum of (*S*,*R*,*R*,*R*)-**Me$_2$DAP**Pt(GpG) suggests that no significant population of an HT conformer exists. The 5′-*cis*-*R* ^{31}P NMR shift (−3.05 ppm) is relatively downfield, suggesting no significant ΔHT1 population (typical ^{31}P NMR shift is about −4.8 ppm). The ΛHT2 conformer has not been observed for any *cis*-PtA_2(GpG) or *cis*-PtA_2(d(GpG)) complex at pH ∼4.5, suggesting that no significant population of a 5′-*cis*-*R* ΛHT2 conformer exists. Furthermore, each HT conformer would have potential interligand clashes between one G O6 and the *cis* N−Me group (Figure 2). A 5′-*cis*-*R* HH2 conformer would have no obvious interligand clashes (Figure 2); MMD calculations predicted that the *anti*, *anti* HH2 conformer of 5′-*cis*-*R* would be ∼2 kcal/mol more stable than that of 5′-*cis*-*S* (Supporting Information), although we emphasize that such energy differences must be interpreted with caution.

A mixture of HH1 and HH2 conformers for 5′-*cis*-*R* (*S*,*R*,*R*,*R*)-**Me$_2$DAP**Pt(GpG) could explain the observation that the 5′-G H8 signal, which is somewhat upfield, is broader than the 3′-G H8 signal, which is downfield (Table 1). MMD calculations (Table 3) predict that an HH1 variant would have little or no canting because of potential steric clashes between the O6 of a canted G and the N−Me groups of the **Me$_2$DAP** ligand. In contrast, the lowest energy HH2 variant (Supporting Information) had the 5′-G canted (i.e., HH2 R). Thus, for such a HH1 and HH2 R mixture, the 3′-G base would be uncanted in either case, explaining the downfield shift. The 5′-G base would be exchanging between a canted (downfield shift) and

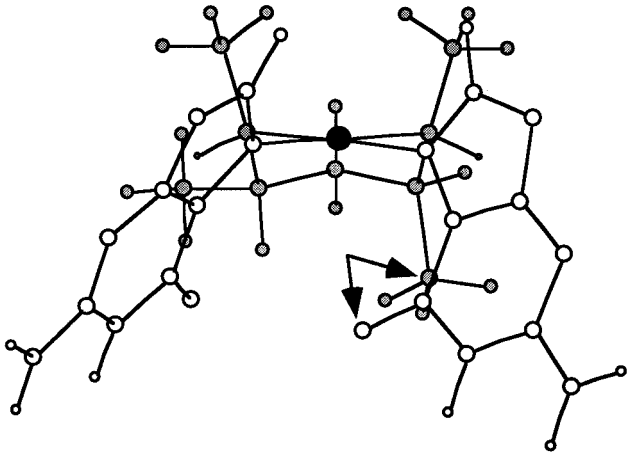

Figure 12. Lowest-energy MMD calculated structure of (*S*,*S*,*S*,*R*)-**Me$_2$DAP**Pt(GpG) with the **Me$_2$DAP** ligand (shown in gray) in the δ-chair conformation. The phosphodiester backbone is omitted for clarity. Arrows designate the 3′-G O6 and C^5 atoms.

an uncanted (upfield shift) position; thus, the 5′-G H8 signal would have an intermediate shift and would exhibit exchange broadening, as observed. Thus, it appears possible that the 5′-*cis*-*R* isomer conformer mixture contains some of an HH2 conformer.

For (*S*,*S*,*S*,*S*)-**Me$_2$DAP**Pt(GpG), multiple sets of broad H8 features (Figure 9) and the presence of two ^{31}P NMR signals indicate that exchange between conformers is moderately slow on the NMR time scale. The broad upfield H8 signal (Figure 9) and the upfield ^{31}P signal at ca. −4.8 ppm indicate the presence of a significant population (∼50%) of the ΔHT1 conformer. The CD spectra at both low and high pH (Figure 10) are similar to those of (*S*,*R*,*R*,*S*)-**Bip**Pt(GpG),[5] supporting the presence of a significant population of a ΔHT1 conformer of (*S*,*S*,*S*,*S*)-**Me$_2$DAP**Pt(GpG). This conformer would be favored by the absence of steric clashes compared to the HH1 variants in which steric clashes between the 3′-G O6 and the C^{4}Me group (δ-chair conformation) or the N^{4}Me group (λ-chair and δ-skew conformations, Figure 3) are expected.

For the (*S*,*S*,*S*,*R*)-**Me$_2$DAP** ligand, MMD calculations predict that the δ-chair conformation is favored (Table 3). (*S*,*S*,*S*,*R*)-**Me$_2$DAP**Pt(GpG) has broad H8 resonances (Supporting Information), indicating a mixture of conformers exchanging at a moderate rate for both linkage isomers. The ^{1}H NMR and CD spectra have features indicative of a significant population of the ΔHT1 conformer for both linkage isomers (Supporting Information). Thus, (*S*,*R*,*R*,*R*)- and (*S*,*S*,*S*,*R*)-**Me$_2$DAP**Pt(GpG) favor different conformer distributions; this finding demonstrates that the stereochemistries of the carbon atoms influence the conformer distributions for these complexes. Unfavorable interactions between a G O6 atom and the *cis* C-Me group were suggested previously for [**Me$_2$DAP**Pt(9-EtG)$_2$]$^{2+}$ complexes.[17] For (*S*,*S*,*S*,*R*)-**Me$_2$DAP**Pt(GpG), clashes between the 3′-G O6 and the C^{4}Me group are possible for the HH1 R variant of the 5′-*cis*-*S* isomer (Figure 12). In the 5′-*cis*-*R* linkage isomer, the G O6 atoms and the N−Me groups would be on the same side of the coordination plane for the HH1 conformer (Figure 2), and canting of either base would result in clashes.

When the pH of a sample of (*R*,*R*,*R*,*R*)-**Me$_2$DAP**Pt(GpG) was raised to 9.5, the **Me$_2$DAP** ligand isomerized (Figure 11). Three **Me$_2$DAP** configurations are possible: *R*,*R*,*R*,*R*, *S*,*R*,*R*,*S*, and *S*,*R*,*R*,*R*. For the adduct with the last configuration, two linkage isomers are possible. The dominant product was the 5′-*cis*-*S* isomer of (*S*,*R*,*R*,*R*)-**Me$_2$DAP**Pt(GpG), demonstrating that this isomer is thermodynamically favored when N1 is deprotonated. However, MMD calculations on the N1 protonated form (Table 3) and the relatively upfield shift of the N^{4}H signal at pH 4 (Table 2) suggest that this isomer does not form an amine−O6 hydrogen bond; thus, the stabilities of **Me$_2$DAP**Pt(GpG) complexes are influenced more by steric than by hydrogen-bonding interactions. Furthermore, the favored isomer had the sharpest NMR signals of any isomer at room temperature. Thus, the favored isomer is also the least dynamic one.

Isomerization of the **Me$_2$DAP** ligand occurred over time also for (*S*,*S*,*S*,*R*)-**Me$_2$DAP**Pt(GpG) at pH 9.5 (Supporting Information). The exact distribution of isomers that formed could not be determined because of the broadness of the H8 signals; however, signals corresponding to (*S*,*S*,*S*,*S*)-**Me$_2$DAP**Pt(GpG) and to at least one linkage isomer of (*S*,*S*,*S*,*R*)-**Me$_2$DAP**Pt(GpG) were present. Thus, while (*R*,*R*,*R*,*R*)-**Me$_2$DAP**Pt(GpG) isomerized to one major product (Figure 11), (*S*,*S*,*S*,*S*)-**Me$_2$DAP**Pt(GpG) gave a mixture. These results indicate that steric interligand interactions influence the thermodynamic stabilities of the various **Me$_2$DAP**Pt(GpG) isomers.

For **Bip**Pt(GpG) complexes, the **Bip** stereochemistry controlled the conformer distribution and the handedness of the canting.[5] In energy-minimized MMD structures, the canting resulted in the formation of amine−O6 hydrogen bonds. Furthermore, the observed HT conformers could form two amine−O6 hydrogen bonds; these conformers became more favored at high pH, and this was attributed to O6 becoming a better hydrogen bond acceptor when N1 was deprotonated. However, many **Me$_2$DAP**Pt(GpG) complexes have carrier ligand bulk that is significantly out of the platinum coordination plane. Steric interligand clashes can occur between the G O6 atoms and an axial N−Me or C−Me group; such clashes alter the conformer distribution. Thus, both favorable hydrogen bonding interactions and unfavorable steric interactions can influence the conformer distribution and the dynamic properties of *cis*-PtA$_2$(GpG) and (presumably) *cis*-PtA$_2$(d(GpG)) cross-links. These interactions also influence the degree of base canting.

Acknowledgment. This work was supported by NIH Grant GM 29222 to L.G.M., NATO CRG 950376 to L.G.M. and G.N., and MURST (contribution 40%), CNR, and EC (COST Chemistry Project D8/0012/97) to G.N.

Supporting Information Available: Procedure for NMR signal assignments; table of calculated minimum energies of **Me$_2$DAP**Pt(GpG) with the GpG ligand fixed; table of energies of fully minimized structures of HH1, HH2, ΔHT1, and ΛHT2 conformers; partial NOESY spectra of (*R*,*R*,*R*,*R*)- and (*S*,*R*,*R*,*R*)-**Me$_2$DAP**Pt(GpG); H8 and **Me$_2$DAP** regions of ^{1}H NMR spectra of (*S*,*S*,*S*,*S*)- and (*S*,*S*,*S*,*R*)-**Me$_2$DAP**Pt(GpG) and isomerized products; ^{1}H NMR spectra of early stages of the formation reactions of (*S*,*R*,*R*,*R*)- and (*R*,*R*,*R*,*R*)-**Me$_2$DAP**Pt(GpG); ^{1}H NMR spectra of (*R*,*R*,*R*,*R*)- **Me$_2$DAP**Pt(GpG) at pH 9 over time; CD spectra of (*R*,*R*,*R*,*R*)-**Me$_2$DAP**Pt(GpG) at pH 4.5 and before and after 2 h at pH 9.4; partial **Me$_2$DAP** region of the ^{1}H NMR spectra of (*R*,*R*,*R*,*R*)-**Me$_2$DAP**Pt(GpG) at various temperatures; and stereoviews of lowest-energy MMD calculated structures of (*R*,*R*,*R*,*R*)-**Me$_2$DAP**Pt(GpG). This material is available free of charge via the Internet at http://pubs.acs.org.

IC000067N